Non-Linear Thermovoltage in a Single-Electron Transistor

Paolo A. Erdman, Joonas T. Peltonen, Bibek Bhandari, Bivas Dutta, Hervé Courtois, Rosario Fazio, Fabio Taddei, Jukka P. Pekola

Nonlinear thermovoltage in a single-electron transistor

P. A. Erdman,[1,*] J. T. Peltonen,[2] B. Bhandari,[1] B. Dutta,[3] H. Courtois,[3] R. Fazio,[4,1] F. Taddei,[5] and J. P. Pekola[2]

[1]*NEST, Scuola Normale Superiore and Istituto Nanoscienze-CNR, I-56127 Pisa, Italy*

[2]*QTF Centre of Excellence, Department of Applied Physics, Aalto University School of Science, P.O. Box 13500, 00076 Aalto, Finland*

[3]*Univ. Grenoble Alpes, CNRS, Institut Néel, 25 Avenue des Martyrs, 38042 Grenoble, France*

[4]*ICTP, Strada Costiera 11, I-34151 Trieste, Italy*

[5]*NEST, Istituto Nanoscienze-CNR and Scuola Normale Superiore, I-56126 Pisa, Italy*

(Received 18 December 2018; revised manuscript received 17 March 2019; published 2 April 2019)

We perform direct thermovoltage measurements in a single-electron transistor, using on-chip local thermometers, in both the linear and nonlinear regimes. Using a model which accounts for cotunneling, we find excellent agreement with the experimental data with no free parameters even when the temperature difference is larger than the average temperature (far-from-linear regime). This allows us to confirm the sensitivity of the thermovoltage on cotunneling and to find that in the nonlinear regime the temperature of the metallic island is a crucial parameter. Surprisingly, the metallic island tends to overheat even at zero net charge current, resulting in a reduction of the thermovoltage.

DOI: 10.1103/PhysRevB.99.165405

I. INTRODUCTION

The use of nanodevices has emerged as one of the key technologies in the quest to establish a sustainable energy system, allowing at the same time the control of heat flow in small circuits [1]. So far, most of the investigations of thermal properties in nanostructures have focused on the thermal conductance [2–11]. Conversely the thermovoltage, which describes the electrical response to a temperature difference and is directly related to both the power and efficiency of thermal machines [1], is much less studied. This is due to the difficulty in coupling local sensitive electron thermometers and heaters/coolers to the sample under study in order to have a well-defined, known temperature difference across the device. The thermovoltage has been measured in devices based on nanowires [12,13] and on quantum dots [14–26]. In these experiments, however, the temperatures of the electrodes were typically not measured directly, but rather determined as fitting parameters, and there are no experiments where the temperature of the electrodes and the thermovoltage are measured simultaneously. Furthermore, there are no experiments probing the thermovoltage in devices based on metallic islands, while theoretical works for these systems have focused only on the linear response regime [27–33]. The nonlinear thermovoltage though has been theoretically studied in discrete-level systems in Refs. [34–43].

In this paper, we report on the measurement of the thermovoltage in a metallic single-electron transistor (SET) using on-chip, local tunnel-junction-based thermometers and electron temperature control. This system allows us to perform thermoelectric measurements with an unprecedented control, within both the linear and nonlinear response regimes, imposing temperature differences exceeding the average temperature. Using a theoretical model which accounts for nonlinear effects and cotunneling processes, we find an excellent agreement with the experimental data with no free parameters. On one hand, this allows us to nail down quantitatively the role of cotunneling processes on the thermovoltage. On the other hand, we find that in the nonlinear regime the temperature of the island emerges as a crucial parameter. Surprisingly, although the thermovoltage is measured at zero net charge current, within the nonlinear response the island tends to overheat to a temperature greater than the average lead temperature, which results in a suppression of the thermovoltage. We show, however, that the nonlinear thermovoltage can be optimized up to a factor of 2 with respect to the experimentally observed value by lowering the temperature of the island to the temperature of the cold lead. This could be achieved by exploiting the phonons in the island which act as a third thermal bath coupled to our system.

II. EXPERIMENTAL SETUP

Figure 1(a) is a colored scanning electron micrograph of the device and Fig. 1(b) is a schematic representation of the experiment with the same colors highlighting the main elements of the fully normal-conducting SET. The left lead L (red) and the right lead R (green) are tunnel and capacitively coupled to a central metallic island I (yellow), which is under the influence of a tunable gate electric field (orange). A voltage bias, $V_b = V_L - V_R$, can be applied to the SET electrodes and the corresponding current I can be measured for an initial characterization of the device. The temperature T_R of the electrons in R is fixed to the bath temperature, given the strong electron-phonon coupling in the large and "bulky" lead. On the other hand, the electronic temperature T_L in the left lead (red) can both be varied and measured using the superconducting tunnel probes (blue). The tunability of the temperature is possible thanks to the superconducting wire (purple) in

*paolo.erdman@sns.it

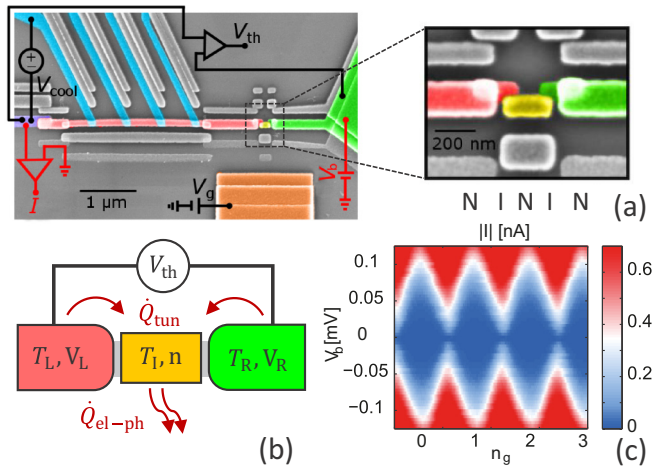

FIG. 1. Representation and characterization of the single-electron transistor. (a) False-colored scanning electron microscopy (SEM) image of the full device and a zoomed-in view around the metallic island (yellow) tunnel coupled to two normal leads (red and green). (b) Schematic representation of the system with the same coloring as in the SEM image. The heat balance in the metallic island is represented by red arrows. (c) Absolute value of the current through the SET as a function of the applied source drain voltage V_b and of the gate-induced charge n_g.

clean contact with the left lead through which there is no heat conduction and thanks to the limited size of the normal (red) part of the lead that reduces the electron-phonon heat flux. Electrons within the island are in local equilibrium at temperature T_I since the electron-electron interaction is much faster than the tunneling rates [44]. The experiment is performed in a dilution refrigerator at bath temperatures typically between 50 and 400 mK. For the thermovoltage measurements, the SET voltage bias source and current preamplifier [sketched in red in Fig. 1(a)] are disconnected. Crucially, the thermovoltage V_{th} is probed directly across the SET using a room-temperature voltage preamplifier with ultralow input bias current below 20 fA. Fabrication details can be found in Ref. [9] where "sample B" is the device used for this experiment.

Figure 1(c) shows the absolute value of the current I across the device at 65 mK as a function of the potential bias V_b and of the gate-induced charge $n_g = (C_L V_L + C_R V_R + C_g V_g)/e$, where C_L, C_R, and C_g are, respectively, the capacitances of the island to L, to R and to the gate electrode, and V_g is the gate voltage. In the dark blue regions, Coulomb diamonds, single-electron tunneling between the leads and the island is not allowed, and the current is very small. At half-integer values of n_g, "degeneracy points," there are conductance peaks at zero bias since single-electron tunneling is allowed for any finite-voltage bias.

III. MODEL

The state of the SET is characterized by the probability $P(n)$ to have n excess charges on the island. The electrostatic energy necessary for this is

$$U(n) = E_C(n - n_g)^2, \tag{1}$$

where $E_C = e^2/(2C)$ is the charging energy with $C = C_L + C_R + C_g$. Electron tunneling between the leads and the island induces transitions between charge states. The leading-order process in a perturbative expansion in the tunnel coupling between the island and the leads corresponds to a single-electron transfer between the leads and the island (sequential tunneling) [45,46]. The sequential-tunneling rates for transferring electrons from $\alpha = $ L,R (I) to $\beta = $ I (L,R), with the island initially having n charges, is denoted by $\Gamma_{\alpha\beta}(n)$ (see the Appendix for details).

Higher-order processes can become dominant if all sequential-tunneling processes are energetically unfavorable [in the Coulomb diamond region in Fig. 1(c)]. In particular, cotunneling (second-order process) refers to the transfer of an electron from one lead to another, without changing the charge state of the island but going through a virtual state. The dominant contribution of this kind is inelastic cotunneling, i.e., the electron which tunnels from lead L, say, to I via a virtual state has a different energy with respect to the electron tunneling from I to R [47]. We denote the rate of inelastic cotunneling that transfers a charge from $\alpha = $ L (R) to $\beta = $ R (L), when n electrons are on the island before the process occurs, by $\gamma_{\alpha\beta}(n)$.

The probabilities $P(n)$ can be computed by solving a master equation (see the Appendix for details). The charge current can then be written as $I(V_b) = I^{seq} + I^{cot}$, where

$$I^{seq} = e\sum_n P(n)[\Gamma_{LI}(n) - \Gamma_{IL}(n)] \tag{2}$$

is the sequential-tunneling contribution, given by electrons tunneling between lead L and I, and $I^{cot} = e\sum_n P(n)[\gamma_{LR}(n) - \gamma_{RL}(n)]$ is the inelastic cotunneling contribution [29,30,46,48,49]. We compute the sequential and cotunneling rates exactly, without linearizing in the voltage bias and temperature difference (see the Appendix for details).

In the presence of a fixed temperature bias ($T_R \neq T_L$), the thermovoltage V_{th} is the solution to

$$I(V_{th}) = 0. \tag{3}$$

Notice that the charge current also depends on the temperature of the island T_I. By imposing that the charge current and the net energy entering the island through electron tunneling are zero, we find that

$$T_I = \frac{T_L R_R + T_R R_L}{R_L + R_R}, \tag{4}$$

where R_L and R_R are respectively the resistance of the left and right tunnel junctions. Equation (4), which is found performing a simple sequential tunneling calculation within linear response and in the two charge state approximation (valid for $E_C \gg k_B T$), reduces to $T_I = \bar{T} \equiv (T_L + T_R)/2$ in the present symmetric case where $R_L = R_R$. We will thus initially assume that T_I is given by the average lead temperature $\bar{T}$. However, as we will soon discuss in detail, we find that this assumption gives quantitatively wrong results beyond the linear response regime, leading us to the exploration of the impact of T_I on the thermovoltage.

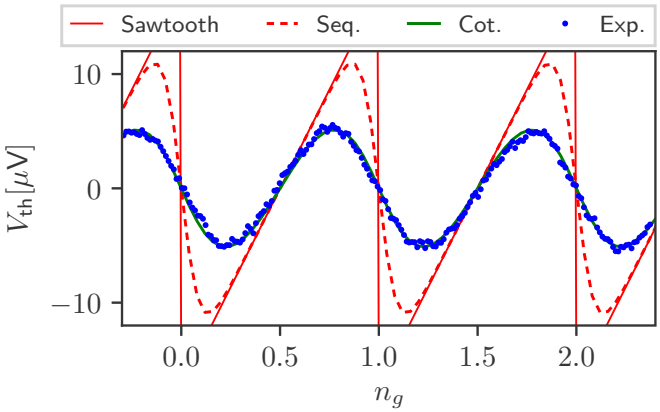

FIG. 2. Experimental and theoretical thermovoltage as a function of n_g. The red thin curve represents the sawtooth behavior predicted with a sequential-tunneling calculation in linear response and accounting for two charge states. The dashed red curve is found by solving Eq. (3) including only sequential contributions, while the green curve includes also cotunneling contributions. The temperatures of the leads are $T_{\rm L} = 134$ mK and $T_{\rm R} = 190$ mK and, according to Eq. (4), we assume that $T_{\rm I} = \bar{T}$.

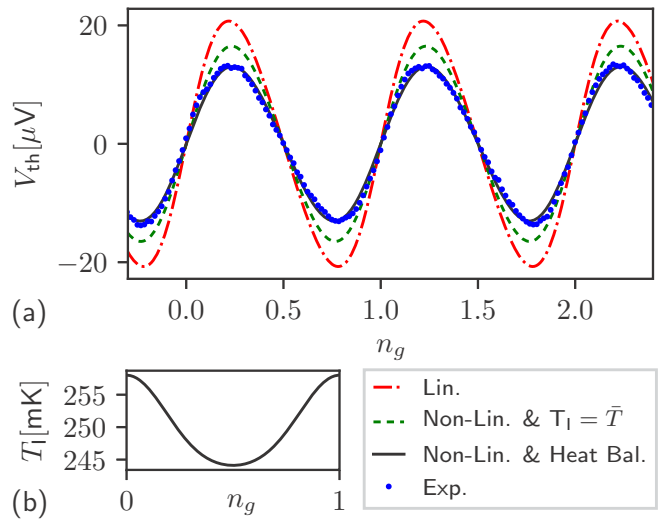

FIG. 3. (a) Experimental and theoretical thermovoltage as a function of n_g. All theoretical curves include cotunneling. The red dashed-dotted curve corresponds to a linear response calculation around $\bar{T}$. The green dashed curve corresponds to a nonlinear calculation where we fix $T_{\rm I} = \bar{T}$, while the black curve corresponds to a nonlinear calculation where $T_{\rm I}$, shown in panel (b) as a function of n_g, is calculated solving the heat balance condition in Eq. (5) together with Eq. (3). The temperatures of the leads are $T_{\rm L} = 342$ mK and $T_{\rm R} = 63$ mK.

IV. RESULTS

We focus on two data sets which represent two different regimes: linear response (Fig. 2), i.e., when the modulus of the temperature difference $\Delta T = T_{\rm L} - T_{\rm R}$ is smaller than the average lead temperature $\bar{T} = (T_{\rm L} + T_{\rm R})/2$, and nonlinear response (Fig. 3). In both cases, using the model detailed above, we could accurately reproduce the experimental data without any free parameter. The system parameters $E_C = 100\ \mu$eV $\approx k_B \times 1.16$ K and $R_{\rm L} = R_{\rm R} = 26$ kΩ are independently extracted from charge current measurements. Figures 2 and 3(a) present the same qualitative behavior, namely, a periodic oscillation of the thermovoltage with the gate-induced charge n_g and a linear dependence around degeneracy points, but they exhibit different amplitudes (note that the sign of $V_{\rm th}$ is opposite in the two cases since the temperature biases are opposite).

We first analyze the linear response regime by choosing the set of data obtained when the temperature of the leads is $T_{\rm L} = 134$ mK and $T_{\rm R} = 190$ mK, such that $|\Delta T| < \bar{T}$. In Fig. 2 we compare the measured $V_{\rm th}$ (blue dots) as a function of n_g with different theoretical models. The red thin curve represents the typical sawtooth behavior which is predicted within linear response accounting only for sequential tunneling and two charge states. This is characterized by a linear function of n_g, crossing zero at the degeneracy points with slope $E_C \Delta T/\bar{T}$ [27]. The other two curves (red dashed and green solid) are instead determined by computing $V_{\rm th}$ using Eq. (3) and assuming that $T_{\rm I} = \bar{T}$ [see Eq. (4)]. The red dashed curve, which only accounts for sequential tunneling, shows a smoothened sawtooth behavior as a consequence of including multiple charge states in the master equation and of a finite temperature. However, both models based on sequential tunneling (thin and dashed red curves) approximately fit the experimental data only near the degeneracy points (near half-integer values of n_g). In this case, indeed, sequential tunneling is allowed and thus dominates over cotunneling [29]. On the other hand the green solid curve, computed including cotunneling contributions, shows a strong suppression of the thermovoltage as we move away from degeneracy points. The excellent agreement between this model and the experimental measurements pinpoints the critical dependence of the thermovoltage on inelastic cotunneling processes.

We now move to the nonlinear regime. In Fig. 3(a) we show the measured thermovoltage as a function of n_g (blue dots) compared to theoretical calculations, all of which include cotunneling contributions. The lead temperatures are $T_{\rm L} = 342$ mK and $T_{\rm R} = 63$ mK, such that $|\Delta T| > \bar{T}$. The red dashed-dotted curve is computed within the linear response regime choosing the average lead temperature $\bar{T}$ as the characteristic temperature. More precisely, we solve Eq. (3) setting $T_{\rm I} = \bar{T}$ and choosing a small temperature difference of the leads δT around $\bar{T}$ to find the thermopower $S \equiv V_{\rm th}/\delta T$ for $\delta T \to 0$. We then calculate the thermovoltage as $V_{\rm th} = S(T_{\rm L} - T_{\rm R})$, where now $T_{\rm L} = 342$ mK and $T_{\rm R} = 63$ mK are the actual lead temperatures. As we can see from Fig. 3(a), this linear response model overestimates the thermovoltage almost by a factor of 2. A nonlinear calculation (green dashed curve) improves the agreement with the experimental data. This calculation is performed by solving Eq. (3) using the actual lead temperatures and, as before, we fix the island temperature at $T_{\rm I} = \bar{T}$. The difference between the red dashed-dotted and green dashed curves proves that we are indeed in the nonlinear response regime, and it shows that the main effect of the nonlinear response is to decrease the amplitude of the thermovoltage. However, we still do not obtain a good agreement with the experimental data.

We find that we can get a perfect agreement with the experimental data if we further improve the model by

determining also the island temperature T_I through a heat balance equation, rather than fixing it at $\bar{T}$. More precisely [see Fig. 1(b)], we denote by $\dot{Q}_{tun}$ the heat current entering the island from sequential and cotunneling events (see the Appendix for details) and by $Q_{el\text{-}ph} = \Sigma\mathcal{V}(T_I^5 - T_R^5)$ the heat current flowing from electrons in the island to the phonons (we assume that the electronic temperature T_R in the bulky right electrode is equal to the temperature of the phonons). $\mathcal{V}$ is the island volume and Σ is the electron-phonon coupling constant which only depends on the material. The temperature of the island can thus be determined by the following heat balance equation:

$$\dot{Q}_{tun} = \dot{Q}_{el\text{-}ph}. \tag{5}$$

The values of the parameters entering $Q_{el\text{-}ph}$ that we use are determined independently: $\mathcal{V} = 225 \times 100 \times 29$ nm^3 is estimated from SEM images and Σ is obtained from Ref. [9] for this device (sample B). The value, $\Sigma = 2.8$ WK^{-5} m^{-3}, is close to the standard literature value for copper [44] and is in agreement with measurements of other samples fabricated using the same Cu target.

The black curve in Fig. 3(a) is thus determined by computing both V_{th} and T_I simultaneously by solving Eqs. (3) and (5) without any free parameters for each value of n_g. As we can see, the nonlinear model, complemented with the heat balance equation, is in excellent agreement with the experimental measurements, demonstrating that T_I is indeed an important parameter in the nonlinear regime. Conversely we have verified that, using the parameters of Fig. 2 which are within the linear response regime, V_{th} only weakly depends on the particular choice of T_I between T_L and T_R. In Fig. 3(b) we plot the island temperature T_I, as a function of n_g over a single period, determined in the same calculation that leads to the black curve in Fig. 3(a). Remarkably, despite the very low phonon temperature (63 mK), the calculated $T_I \approx 250$ mK is much larger than the average lead temperature $\bar{T} = 202.5$ mK. This means that while the net charge current across the SET is zero, the heat current due to electrons tunneling back and forth is overheating the island to a temperature that is significantly larger than the average temperature, resulting in a further decrease of the thermovoltage. This is another signature of the nonlinear response of the system, as it violates Eq. (4). We further find that the island temperature displays a weak n_g modulation of approximately 10 mK, but this prediction cannot be confirmed in the present experiment.

Finally we discuss how the thermovoltage depends on T_I. In Fig. 4 we plot V_{th}^{max}, the maximum amplitude of V_{th}, computed by solving Eq. (3) at fixed lead temperatures $T_L = 342$ mK and $T_R = 63$ mK and varying T_I between the lead temperatures. The black solid lines and the gray area point to the actual experimental value of V_{th}^{max} and to the corresponding computed T_I which differs from $\bar{T}$ [see black curves in Figs. 3(a) and 3(b)], while the dashed green lines point to V_{th}^{max} calculated setting $T_I = \bar{T}$ [see the green dashed curve in Fig. 3(a)]. We find that V_{th}^{max} strongly depends on the choice of T_I and that it increases as T_I is lowered. Indeed, at $T_I = T_R = 63$ mK, the amplitude of the thermovoltage reaches 27 μeV, twice the experimental value [see blue dots in Fig. 3(a)]. Thus, by increasing the energy exchange between the electrons and phonons in the island, for example, by increasing the island's volume, we can lower the temperature of the island, which in turn results in an increase of V_{th}.

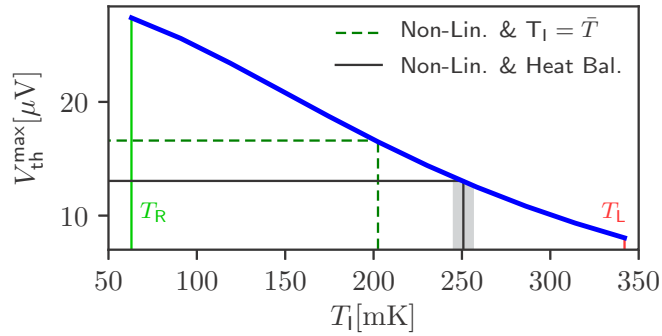

FIG. 4. The maximum amplitude of the thermovoltage V_{th}^{max} is plotted as a function of the island temperature, for $T_R \leqslant T_I \leqslant T_L$. The green dashed lines point to the values of V_{th}^{max} and T_I found in the nonlinear calculation at fixed $T_I = \bar{T}$ [see the green dashed curve of Fig. 3(a)] while the black solid lines and the gray area refer to the nonlinear calculation including the heat balance equation (see the black solid curve of Fig. 3).

V. CONCLUSIONS

We performed measurements of thermovoltage in a metallic island tunnel coupled to normal leads. Within the linear regime we nail down the role of cotunneling in determining the thermovoltage. Within the nonlinear response regime we explore temperature biases, determined with on-chip thermometers, even larger than the average lead temperature. Using a theoretical model which accounts for cotunneling and nonlinear effects, we find an accurate agreement with the experimental data without any free parameters. In particular, we find that the temperature of the metallic island becomes an important parameter which must be determined by solving a heat balance equation for the island. Surprisingly, even if the net charge current through the system is vanishing and the coupling to the leads is symmetric, the metallic island overheats to a temperature larger than the average lead temperature. As a consequence, the amplitude of the thermovoltage oscillations decreases.

ACKNOWLEDGMENTS

This work has been supported by the Academy of Finland (Grant No. 312057), by the European Union's Horizon 2020 research and innovation program under the European Research Council (ERC) program (Grant No. 742559), by the SNS-WIS joint laboratory "QUANTRA," by the SNS internal project "Thermoelectricity in Nano-devices," by the CNR-CONICET cooperation program "Energy Conversion in Quantum, Nanoscale, Hybrid Devices," and by the COST ActionMP1209 program "Thermodynamics in the Quantum Regime." B.D. acknowledges support from the Nanosciences Foundation under the auspices of the Universite Grenoble Alpes Foundation.

APPENDIX: COMPUTING CHARGE AND HEAT CURRENTS

The system is described by the following Hamiltonian:

$$\hat{H} = \sum_{\alpha=\mathrm{L,R}} \hat{H}_\alpha + \hat{H}_\mathrm{I} + \hat{H}_\mathrm{t}, \tag{A1}$$

where $\hat{H}_\alpha = \sum_{k\sigma}(\epsilon_k + eV_\alpha)a^\dagger_{k\sigma\alpha}a_{k\sigma\alpha}$ is the Hamiltonian of the free electrons in lead $\alpha = \mathrm{L,R}$, $\hat{H}_\mathrm{I} = \sum_{k\sigma}\epsilon_k c^\dagger_{k\sigma}c_{k\sigma} + E_C(\hat{n}-n_g)^2$ is the Hamiltonian of the electrons in the metallic island, and $\hat{H}_\mathrm{t} = \sum_{kp\sigma\alpha} t^{(\alpha)}_{kp} c^\dagger_{p\sigma}a_{k\sigma\alpha} + \mathrm{H.c.}$ is the usual tunneling Hamiltonian between the leads and the island. $a_{k\sigma\alpha}$ ($a^\dagger_{k\sigma\alpha}$) is the destruction (creation) operator of electrons in lead α with energy $\epsilon_k + eV_\alpha$ and spin σ, $c_{k\sigma}$ ($c^\dagger_{k\sigma}$) is the destruction (creation) operator of electrons in the metallic island with energy ϵ_k and spin σ, and $\hat{n}$ is the operator for the number of excess electrons on the island.

In order to describe charge and heat transport in the system, we employ a master equation approach to compute the probabilities $P(n)$ in terms of all processes that can induce transitions between charges states (the tunneling rates). Sequential tunneling of electrons between the island and the leads changes the charge state by one, so it enters the master equation. Cotunneling processes instead transfer an electron from one lead to another one via a virtual state in the island, but the overall process does not change the number of electrons in the island; consequently, the master equation does not depend on cotunneling. Second-order processes that transfer two electrons from/to the leads to/from the island can be safely neglected as the charging energy E_C is much larger than the thermal energy k_BT and than the voltage bias range considered in this work. The master equation reads

$$\frac{\partial P(n)}{\partial t} = \sum_{\alpha=L,R}\{-P(n)[\Gamma_{\alpha I}(n) + \Gamma_{I\alpha}(n)] + P(n-1) \times \Gamma_{\alpha I}(n-1) + P(n+1)\Gamma_{I\alpha}(n+1)\}, \tag{A2}$$

and we solve it by setting $\partial P(n)/\partial t = 0$ for every n. Equation (A2) states that the probability of being in charge state n can decrease [first right-hand-side (r.h.s.) term] if the island has n excess charge states and an electron tunnels into or out of the island, while it can increase (second and third r.h.s. terms) if, after a sequential tunneling process, the number of excess charges on the island is n.

Given the probabilities, the charge current can be computed by summing I^seq and I^cot given in Eq. (2) and below. The energy entering the metallic island $\dot{Q}_\mathrm{tun}$ can be computed as

$$\dot{Q}_\mathrm{tun} \equiv I^\mathrm{E}_\mathrm{L} + I^\mathrm{E}_\mathrm{R} = I^\mathrm{h}_\mathrm{L} + I^\mathrm{h}_\mathrm{R} + e(V_\mathrm{L} - V_\mathrm{R})I, \tag{A3}$$

where I^E_α and I^h_α are respectively the energy (measured respect to the common voltage ground) and heat currents leaving reservoir α, and we used the fact that $I^\mathrm{E}_\mathrm{L} = I^\mathrm{h}_\mathrm{L} + eV_\mathrm{L}I$ and $I^\mathrm{E}_\mathrm{L} = I^\mathrm{h}_\mathrm{R} - eV_\mathrm{R}I$. We can simply interpret the r.h.s. of Eq. (A3) by noticing that the heat entering the metallic island is given by the sum of the heat leaving the leads and the heat generated by the Joule effect. We notice that a shift of the energy reference shifts V_L and V_R, but it does not change I^h_L and I^h_R, so $\dot{Q}_\mathrm{tun}$, as defined in Eq. (A3), does not depend on the unphysical energy reference.

The heat currents can be calculated in terms of "heat rates." We thus define $\Gamma^h_{\alpha\mathrm{I}}(n)$ as the rate of heat leaving reservoir α when electrons tunnel sequentially from lead α to the island with n initial electrons, and we define $\Gamma^h_{\mathrm{I}\alpha}(n)$ as the rate of heat entering lead α when electrons tunnel sequentially from the island to lead α with n initial electrons. Analogously, we define $\gamma^{h/\mathrm{out}}_{\alpha\beta}(n)$ as the rate of heat leaving lead α when a cotunneling process transfers one electron from lead α to lead β with n electrons in the island, and we define $\gamma^{h/\mathrm{in}}_{\alpha\beta}(n)$ as the rate of heat entering lead β when a cotunneling process transfers one electron from lead α to lead β with n electrons in the island. Notice that also cotunneling processes where $\alpha = \beta$ must be considered in the heat currents, since the electron leaving and the one entering the same lead can have different energies. Also the heat currents can be written as $I^h_\alpha = I^{h/\mathrm{seq}}_\alpha + I^{h/\mathrm{cot}}_\alpha$, where

$$I^{h/\mathrm{seq}} = \sum_n P(n)\big[\Gamma^h_{\alpha\mathrm{I}}(n) - \Gamma^h_{\mathrm{I}\alpha}(n)\big] \tag{A4}$$

is the sequential-tunneling contribution, given by electrons tunneling between lead α and I, and

$$I^{h/\mathrm{cot}}_\alpha = \sum_{n,\beta=\mathrm{L,R}} P(n)\big[\gamma^{h/\mathrm{out}}_{\alpha\beta}(n) - \gamma^{h/\mathrm{in}}_{\beta\alpha}(n)\big] \tag{A5}$$

is the inelastic cotunneling contribution.

Using the T-matrix theory (or generalized Fermi golden rule) [48–50], we can compute sequential and cotunneling rates. The transition rate from a given initial state $|i\rangle$ to a final state $|f\rangle$ is given by

$$\Gamma_{i\to f} = \frac{2\pi}{\hbar} p_i(1-p_f)|\langle f|T|i\rangle|^2\delta(E_f - E_i), \tag{A6}$$

where p_i and p_f are the probabilities of finding the system in state i and state f, E_i and E_f are the energies of states i and f, and $T = \hat{H}_t + \hat{H}_t G_0 \hat{H}_t + \cdots$ is the T matrix with $G_0 = 1/(E_i - \hat{H}_0 + i\eta)$ denoting the Green function in the absence of $\hat{H}_t$, i.e., $\hat{H}_0 = \hat{H}_\mathrm{L} + \hat{H}_\mathrm{R} + \hat{H}_\mathrm{I}$. We compute sequential rates by taking T at first order in $\hat{H}_t$. We thus take $T = \hat{H}_t$ in Eq. (A6) and sum over all states in the lead and in the island, yielding

$$\Gamma_{\alpha I}(n) = \frac{2\pi}{\hbar}\sum_{k_1\sigma_1,k_2\sigma_2} f_\alpha(\epsilon_{k_1}) f^-_I(\epsilon_{k_2})\big|\langle 0|c_{k_2\sigma_2}H_t a^\dagger_{k_1\sigma_1\alpha}|0\rangle\big|^2 \times \delta\big[\epsilon_{k_2} - \epsilon_{k_1} + \Delta E_\alpha(n)\big], \tag{A7}$$

where $\Delta E_\alpha(n) = U(n+1) - U(n) - eV_\alpha$ is the electrostatic energy difference to move an electron from lead α to the island, $f_{\alpha/\mathrm{I}}(\epsilon) = \{1 + \exp[\epsilon/(k_BT_{\alpha/I})]\}^{-1}$ is the Fermi distribution of lead α at temperature T_α or of the island at temperature T_I, $f^-_{\alpha/\mathrm{I}}(\epsilon) = f_{\alpha/\mathrm{I}}(-\epsilon) = 1 - f_{\alpha/\mathrm{I}}(\epsilon)$, and k_B is the Boltzmann constant. An analogous expression holds for $\Gamma_{I\alpha}(n)$. The heat rates are computed in the same way, taking into account that an amount of heat ϵ_k is removed(injected) from(into) a lead if an electron with momentum k tunnels

from (into) the lead. We thus have that

$$\Gamma^h_{\alpha I}(n) = \frac{2\pi}{\hbar}\sum_{k_1\sigma_1,k_2\sigma_2} \epsilon_{k_1} f_\alpha(\epsilon_{k_1}) f_I^-(\epsilon_{k_2}) \left|\langle 0|c_{k_2\sigma_2} H_t a^\dagger_{k_1\sigma_1\alpha}|0\rangle\right|^2 \times \delta\left[\epsilon_{k_2} - \epsilon_{k_1} + \Delta E_\alpha(n)\right],$$

$$\Gamma^h_{I\alpha}(n) = \frac{2\pi}{\hbar}\sum_{k_1\sigma_1,k_2\sigma_2} \epsilon_{k_2} f_I(\epsilon_{k_1}) f_\alpha^-(\epsilon_{k_2}) \left|\langle 0|a_{k_2\sigma_2\alpha} H_t c^\dagger_{k_1\sigma_1}|0\rangle\right|^2 \times \delta\left[\epsilon_{k_2} - \epsilon_{k_1} - \Delta E_\alpha(n-1)\right]. \quad \text{(A8)}$$

By assuming that the energy levels in the leads and in the island form a continuum, by taking a constant density of states around the Fermi energy, and by replacing the hopping parameters $t^{(\alpha)}_{kp}$ with their averaged value over k and p, we can write the sequential rates and heat rates in terms of the functions

$$\Upsilon_\alpha(\Delta E) \equiv \frac{1}{e^2 R_\alpha}\int_{-\infty}^{+\infty} d\epsilon f_\alpha(\epsilon) f_I^-(\epsilon - \Delta E),$$

$$\Upsilon^h_\alpha(\Delta E) \equiv \frac{1}{e^2 R_\alpha}\int_{-\infty}^{+\infty} d\epsilon\, \epsilon f_\alpha(\epsilon) f_I^-(\epsilon - \Delta E), \quad \text{(A9)}$$

where R_α is the tunnel resistance between lead α and the island, as follows:

$$\Gamma_{\alpha I}(n) = \Upsilon_\alpha[\Delta E_\alpha(n)], \quad \Gamma_{I\alpha}(n+1) = \Upsilon_\alpha[-\Delta E_\alpha(n)],$$
$$\Gamma^h_{\alpha I}(n) = \Upsilon^h_\alpha[\Delta E_\alpha(n)], \quad \Gamma^h_{I\alpha}(n+1) = -\Upsilon^h_\alpha[-\Delta E_\alpha(n)]. \quad \text{(A10)}$$

Cotunneling rates are second-order processes that involve initial and final states with two electrons, so we now consider $T = \hat{H}_t G_0 \hat{H}_t$. We thus take $|i\rangle = a^\dagger_{k_1\sigma_1\alpha} c^\dagger_{q_1\tau_1}|0\rangle$ and $|f\rangle = a^\dagger_{q_2\tau_2\beta} c^\dagger_{k_2\sigma_2}|0\rangle$, which corresponds to considering the process where an electron in state $k_1\sigma_1$ tunnels from lead α to the island into state $k_2\sigma_2$, and another one coherently tunnels from the island in state $q_1\tau_1$ to lead β into state $q_2\tau_2$. From Eq. (A6) we have that

$$\gamma_{\alpha\beta}(n) = \frac{2\pi}{\hbar}\sum_{\substack{k_1\sigma_1,\,k_2\sigma_2\\ q_1\tau_1,\,q_2\tau_2}} f_\alpha(\epsilon_{k_1}) f_I(\epsilon_{q_1}) f_\beta^-(\epsilon_{q_2}) f_I^-(\epsilon_{k_2}) \times \left|\sum_\nu \frac{\langle f|H_t|\nu\rangle\langle\nu|H_t|i\rangle}{E_i - E_\nu + i\eta}\right|^2 \delta\left[\epsilon_{q_2} + \epsilon_{k_2} - \epsilon_{q_1} - \epsilon_{k_1} + e(V_\beta - V_\alpha)\right], \quad \text{(A11)}$$

where $E_i = \epsilon_{q_1} + \epsilon_{k_1} + eV_\alpha + U(n)$ is the energy of state $|i\rangle$, the sum over $|\nu\rangle$ runs over a complete set of eigenstates $\{|\nu\rangle\}$ of H_0, and E_ν is the energy, evaluated with H_0, of state $|\nu\rangle$. As we did for the sequential rates, we notice that in the processes described in Eq. (A11), the heat leaving reservoir α is ϵ_{k_1}, while the heat entering reservoir β is ϵ_{q_2}. The cotunneling heat rate leaving reservoir α, $\gamma^{h/\text{out}}_{\alpha\beta}(n)$, is thus given by Eq. (A11), adding an ϵ_{k_1} inside the sum over the initial and final states, while the cotunneling heat rate entering reservoir β, $\gamma^{h/\text{in}}_{\alpha\beta}(n)$, is also given by Eq. (A11), adding an ϵ_{q_2} inside the sum over the initial and final states. Manipulating Eq. (A11) using the same approximations mentioned for the sequential rates, we find that by defining

$$\upsilon_{\alpha\beta}(\Delta E, \Delta E_1, \Delta E_2) = \frac{\hbar}{2\pi}\int_{-\infty}^{+\infty} d\epsilon \Upsilon_\alpha(-\epsilon)\Upsilon_\beta(\epsilon + \Delta E)\left|\frac{1}{\epsilon + \Delta E_1 - i\eta} - \frac{1}{\epsilon - \Delta E_2 + \Delta E + i\eta}\right|^2,$$

$$\upsilon^{h/\text{out}}_{\alpha\beta}(\Delta E, \Delta E_1, \Delta E_2) = \frac{\hbar}{2\pi}\int_{-\infty}^{+\infty} d\epsilon \Upsilon^h_\alpha(-\epsilon)\Upsilon_\beta(\epsilon + \Delta E)\left|\frac{1}{\epsilon + \Delta E_1 - i\eta} - \frac{1}{\epsilon - \Delta E_2 + \Delta E + i\eta}\right|^2,$$

$$\upsilon^{h/\text{in}}_{\alpha\beta}(\Delta E, \Delta E_1, \Delta E_2) = -\frac{\hbar}{2\pi}\int_{-\infty}^{+\infty} d\epsilon \Upsilon_\alpha(-\epsilon)\Upsilon^h_\beta(\epsilon + \Delta E)\left|\frac{1}{\epsilon + \Delta E_1 - i\eta} - \frac{1}{\epsilon - \Delta E_2 + \Delta E + i\eta}\right|^2, \quad \text{(A12)}$$

we can write the cotunneling rates and heat rates as

$$\gamma_{\alpha\beta}(n) = \upsilon_{\alpha\beta}[e(V_\beta - V_\alpha), \Delta U_\alpha(n), -\Delta U_\beta(n-1)], \quad \text{(A13)}$$

$$\gamma^{h/\text{out}}_{\alpha\beta}(n) = \upsilon^{h/\text{out}}_{\alpha\beta}[e(V_\beta - V_\alpha), \Delta U_\alpha(n), -\Delta U_\beta(n-1)], \quad \text{(A14)}$$

$$\gamma^{h/\text{in}}_{\alpha\beta}(n) = \upsilon^{h/\text{in}}_{\alpha\beta}[e(V_\beta - V_\alpha), \Delta U_\alpha(n), -\Delta U_\beta(n-1)]. \quad \text{(A15)}$$

At last, we notice that the integrals in Eq. (A12) are divergent in the limit $\eta \to 0^+$. In order to overcome this problem, we adopt a commonly used "regularization scheme" [29,30,46,48,49]. All three integrals can be written in the form

$$\mathcal{I} = \int_{-\infty}^{+\infty} d\epsilon g(\epsilon)\left|\frac{1}{\epsilon - \alpha_1 - i\eta} - \frac{1}{\epsilon - \alpha_2 + i\eta}\right|^2 = \sum_{i=1,2}\left\{\int_{-\infty}^{+\infty} d\epsilon g(\epsilon)\left|\frac{1}{\epsilon - \alpha_i - i\eta}\right|^2\right\} - 2\int_{-\infty}^{+\infty} d\epsilon g(\epsilon)\,\mathrm{Re}\left\{\frac{1}{(\epsilon - \alpha_1 + i\eta)(\epsilon - \alpha_2 + i\eta)}\right\} = \sum_{i=1,2}\{\mathcal{I}^{(1)}_i\} - 2\mathcal{I}^{(2)}, \quad \text{(A16)}$$

where $g(\epsilon)$ is a suitable function and α_1 and α_2 are suitable constants. We now analyze each integral:

$$\begin{aligned}\mathcal{I}_i^{(1)} &= \int_{-\infty}^{+\infty} d\epsilon g(\epsilon)\left|\frac{1}{\epsilon-\alpha_i-i\eta}\right|^2 = \int_{-\infty}^{+\infty} d\epsilon \frac{g(\epsilon)-g(\alpha_i)+g(\alpha_i)}{(\epsilon-\alpha_i)^2+\eta^2} \\ &= g(\alpha_i)\int_{-\infty}^{+\infty} d\epsilon \frac{1}{(\epsilon-\alpha_i)^2+\eta^2} + \int_{-\infty}^{+\infty} d\epsilon \frac{g(\epsilon)-g(\alpha_i)}{(\epsilon-\alpha_i)^2+\eta^2} \\ &= \frac{\pi g(\alpha_i)}{\eta} + \mathcal{P}\int_{-\infty}^{+\infty} d\epsilon \frac{g(\epsilon)-g(\alpha_i)}{(\epsilon-\alpha_i)^2} + O(\eta), \end{aligned} \tag{A17}$$

where $\mathcal{P}$ denotes a principal value integration. We notice that the last step of Eq. (A17) is an expansion for small η. In particular, the first term diverges as $1/\eta$, the second one is finite and independent of η, while the third one goes to zero if $\eta \to 0$. The regularization scheme consists of dropping the divergent term and retaining only the second term, which is finite and independent of η:

$$\mathcal{I}_i^{(1)} \to \mathcal{P}\int_{-\infty}^{+\infty} d\epsilon \frac{g(\epsilon)-g(\alpha_i)}{(\epsilon-\alpha_i)^2}. \tag{A18}$$

Let us now turn to

$$\begin{aligned}\mathcal{I}^{(2)} &= \int_{-\infty}^{+\infty} d\epsilon g(\epsilon)\,\mathrm{Re}\left\{\frac{1}{(\epsilon-\alpha_1+i\eta)(\epsilon-\alpha_2+i\eta)}\right\} \\ &= \int_{-\infty}^{+\infty} d\epsilon g(\epsilon)\frac{(\epsilon-\alpha_1)(\epsilon-\alpha_2)-\eta^2}{[(\epsilon-\alpha_1)(\epsilon-\alpha_2)-\eta^2]^2+\eta^2[(\epsilon-\alpha_1)+(\epsilon-\alpha_2)]^2} \\ &= \int_{-\infty}^{+\infty} d\epsilon g(\epsilon)\frac{(\epsilon-\alpha_1)(\epsilon-\alpha_2)-\eta^2}{(\epsilon-\alpha_1)^2(\epsilon-\alpha_2)^2+\eta^2[(\epsilon-\alpha_1)^2+(\epsilon-\alpha_2)^2+\eta^2]}. \end{aligned} \tag{A19}$$

We notice that the denominator in Eq. (A19) is always positive and non-zero. In the limit $\eta \to 0$, the term proportional to $(\epsilon-\alpha_1)(\epsilon-\alpha_2)$ turns into a principal value integration, while the term proportional to $-\eta^2$ vanishes. The regularization scheme thus consists of

$$\mathcal{I}^{(2)} \to \mathcal{P}\int_{-\infty}^{+\infty} d\epsilon \frac{g(\epsilon)}{(\epsilon-\alpha_1)(\epsilon-\alpha_2)}, \tag{A20}$$

which is now finite and independent of η.

[1] G. Benenti, G. Casati, K. Saito, and R. S. Whitney, Phys. Rep. **694**, 1 (2017).

[2] L. W. Molenkamp, T. Gravier, H. van Houten, O. J. A. Buijk, M. A. A. Mabesoone, and C. T. Foxon, Phys. Rev. Lett. **68**, 3765 (1992).

[3] K. Schwab, E. Henriksen, J. Worlock, and M. L. Roukes, Nature (London) **404**, 974 (2000).

[4] O. Chiatti, J. T. Nicholls, Y. Y. Proskuryakov, N. Lumpkin, I. Farrer, and D. A. Ritchie, Phys. Rev. Lett. **97**, 056601 (2006).

[5] M. Meschke, W. Guichard, and J. P. Pekola, Nature (London) **444**, 187 (2006).

[6] E. A. Hoffmann, H. A. Nilsson, J. E. Matthews, N. Nakpathomkun, A. I. Persson, L. Samuelson, and H. Linke, Nano Lett. **9**, 779 (2009).

[7] S. Jezouin, F. D. Parmentier, A. Anthore, U. Gennser, A. Cavanna, Y. Jin, and F. Pierre, Science **342**, 601 (2013).

[8] M. Banerjee, M. Heiblum, A. Rosenblatt, Y. Oreg, D. E. Feldman, A. Stern, and V. Umansky, Nature (London) **545**, 75 (2017).

[9] B. Dutta, J. T. Peltonen, D. S. Antonenko, M. Meschke, M. A. Skvortsov, B. Kubala, J. König, C. B. Winkelmann, H. Courtois, and J. P. Pekola, Phys. Rev. Lett. **119**, 077701 (2017).

[10] L. Cui, W. Jeong, S. Hur, M. Matt, J. C. Klöckner, F. Pauly, P. Nielaba, J. C. Cuevas, E. Meyhofer, and P. Reddy, Science **355**, 1192 (2017).

[11] N. Mosso, U. Drechsler, F. Menges, P. Nirmalraj, S. Karg, H. Riel, and B. Gotsmann, Nat. Nanotechnol. **12**, 430 (2017).

[12] S. Roddaro, D. Ercolani, M. A. Safeen, S. Suomalainen, F. Rossella, F. Giazotto, L. Sorba, and F. Beltram, Nano Lett. **13**, 3638 (2013).

[13] P. M. Wu, J. Gooth, X. Zianni, S. F. Svensson, J. G. Gluschke, K. A. Dick, C. Thelander, K. Nielsch, and H. Linke, Nano Lett. **13**, 4080 (2013).

[14] A. S. Dzurak, C. G. Smith, M. Pepper, D. Ritchie, J. Frost, G. Jones, and D. Hasko, Solid State Commun. **87**, 1145 (1993).

[15] A. A. M. Staring, L. W. Molenkamp, B. W. Alphenaar, H. van Houten, O. J. A. Buyk, M. A. A. Mabesoone, C. W. J. Beenakker, and C. T. Foxon, Europhys. Lett. **22**, 57 (1993).

[16] L. Molenkamp, A. A. M. Staring, B. W. Alphenaar, H. van Houten, and C. W. J. Beenakker, Semicond. Sci. Technol. **9**, 903 (1994).

[17] A. S. Dzurak, C. G. Smith, C. H. W. Barnes, M. Pepper, L. Martín-Moreno, C. T. Liang, D. A. Ritchie, and G. A. C. Jones, Phys. Rev. B **55**, R10197 (1997).

[18] S. Möller, H. Buhmann, S. F. Godijn, and L. W. Molenkamp, Phys. Rev. Lett. **81**, 5197 (1998).
[19] S. F. Godijn, S. Möller, H. Buhmann, L. W. Molenkamp, and S. A. van Langen, Phys. Rev. Lett. **82**, 2927 (1999).
[20] M. C. Llaguno, J. E. Fischer, A. T. Johnson, and J. Hone, Nano Lett. **4**, 45 (2004).
[21] R. Scheibner, H. Buhmann, D. Reuter, M. N. Kiselev, and L. W. Molenkamp, Phys. Rev. Lett. **95**, 176602 (2005).
[22] A. G. Pogosov, M. V. Budantsev, R. A. Lavrov, A. E. Plotnikov, A. K. Bakarov, A. I. Toropov, and J. C. Portal, JETP Lett. **83**, 122 (2006).
[23] R. Scheibner, E. G. Novik, T. Borzenko, M. König, D. Reuter, A. D. Wieck, H. Buhmann, and L. W. Molenkamp, Phys. Rev. B **75**, 041301(R) (2007).
[24] S. F. Svensson, A. I. Persson, E. A. Hoffmann, N. Nakpathomkun, H. A. Nilsson, H. Q. Xu, L. Samuelson, and H. Linke, New J. Phys. **14**, 033041 (2012).
[25] S. F. Svensson, E. A. Hoffmann, N. Nakpathomkun, P. M. Wu, H. Q. Xu, H. A. Nilsson, D. Sánchez, V. Kashcheyevs, and H. Linke, New J. Phys. **15**, 105011 (2013).
[26] B. Dutta, D. Majidi, A. G. Corral, P. Erdman, S. Florens, T. Costi, H. Courtois, and C. B. Winkelmann, Nano Lett. **19**, 506 (2019).
[27] C. W. J. Beenakker and A. A. M. Staring, Phys. Rev. B **46**, 9667 (1992).
[28] A. V. Andreev and K. A. Matveev, Phys. Rev. Lett. **86**, 280 (2001).
[29] M. Turek and K. A. Matveev, Phys. Rev. B **65**, 115332 (2002).
[30] J. Koch, F. von Oppen, Y. Oreg, and E. Sela, Phys. Rev. B **70**, 195107 (2004).
[31] B. Kubala and J. König, Phys. Rev. B **73**, 195316 (2006).
[32] B. Kubala, J. König, and J. Pekola, Phys. Rev. Lett. **100**, 066801 (2008).
[33] A. S. Vasenko, D. M. Basko, and F. W. J. Hekking, Phys. Rev. B **91**, 085310 (2015).
[34] D. Boese and R. Fazio, Europhys. Lett. **56**, 576 (2001).
[35] R. Świrkowicz, M. Wierzbicki, and J. Barnaś, Phys. Rev. B **80**, 195409 (2009).
[36] D. M.-T. Kuo and Y.-C. Chang, Phys. Rev. B **81**, 205321 (2010).
[37] R. López and David Sánchez, Phys. Rev. B **88**, 045129 (2013).
[38] P. Dutt and K. Le Hur, Phys. Rev. B **88**, 235133 (2013).
[39] R. Sánchez, B. Sothmann, A. N. Jordan, and M. Büttiker, New J. Phys. **15**, 125001 (2013).
[40] M. A. Sierra and D. Sánchez, Phys. Rev. B **90**, 115313 (2014).
[41] N. A. Zimbovskaya, J. Chem. Phys. **142**, 244310 (2016).
[42] P. A. Erdman, F. Mazza, R. Bosisio, G. Benenti, R. Fazio, and F. Taddei, Phys. Rev. B **95**, 245432 (2017).
[43] D. Perez Daroca, P. Roura-Bas, and A. A. Aligia, Phys. Rev. B **97**, 165433 (2018).
[44] F. Giazotto, T. T. Heikkilä, A. Luukanen, A. M. Savin, and J. P. Pekola, Rev. Mod. Phys. **78**, 217 (2006).
[45] D. V. Averin and K. K. Likharev, *Mesoscopic Phenomena in Solids* (North-Holland, Amsterdam, 1991).
[46] Y. V. Nazarov and Y. M. Banter, *Quantum Transport* (Cambridge University, Cambridge, England, 2009).
[47] The process where the same electron tunnels from $\alpha = L, R$ to I and then to $\beta = L, R$ is known as "elastic co-tunneling," since also the microscopic state on the island remains unchanged. As discussed in Refs. [33,46], this process is relevant only when the thermal energy k_BT and the voltage bias are much smaller than $\sqrt{E_C\delta}$, where δ is the energy level spacing in the island. In our case the energy levels almost form a continuum, making $\sqrt{E_C\delta}$ the smallest energy scale in play.
[48] K. Kaasbjerg and A.-P. Jauho, Phys. Rev. Lett. **116**, 196801 (2016).
[49] B. Bhandari, G. Chiriacò, P. A. Erdman, R. Fazio, and F. Taddei, Phys. Rev. B **98**, 035415 (2018).
[50] H. Bruus and K. Flensberg, *Many-Body Quantum Theory in Condensed Matter Physics* (Oxford University, New York, 2004).